



HAL
open science

Thermotopes-COH-A software for carbon isotope modeling and speciation of COH fluids

Antoine Boutier, Isabelle Martinez, Isabelle Daniel, Simone Tumiati,
Guillaume Siron, Alberto Vitale Brovarone

► **To cite this version:**

Antoine Boutier, Isabelle Martinez, Isabelle Daniel, Simone Tumiati, Guillaume Siron, et al.. Thermotopes-COH-A software for carbon isotope modeling and speciation of COH fluids. *Computers & Geosciences*, 2024, 184, pp.105533. 10.1016/j.cageo.2024.105533 . hal-04828960

HAL Id: hal-04828960

<https://hal.science/hal-04828960v1>

Submitted on 10 Dec 2024

HAL is a multi-disciplinary open access archive for the deposit and dissemination of scientific research documents, whether they are published or not. The documents may come from teaching and research institutions in France or abroad, or from public or private research centers.

L'archive ouverte pluridisciplinaire **HAL**, est destinée au dépôt et à la diffusion de documents scientifiques de niveau recherche, publiés ou non, émanant des établissements d'enseignement et de recherche français ou étrangers, des laboratoires publics ou privés.



Thermotopes-COH—A software for carbon isotope modeling and speciation of COH fluids

Antoine Boutier^{a,b,c,*}, Isabelle Martinez^c, Isabelle Daniel^b, Simone Tumiatì^d,
Guillaume Siron^{e,f}, Alberto Vitale Brovarone^{f,g,h,**}

^a Dipartimento di Scienze della Terra, Università degli Studi di Torino, Via Valperga Caluso 35, 10100 Torino, Italy

^b Université de Lyon, Univ Lyon 1, ENS de Lyon, CNRS UMR 5276, LGL-TPE, Villeurbanne Cedex, France

^c Université Paris Cité, Institut de Physique du Globe de Paris, CNRS, UMR 7154, F-75005, Paris, France

^d Dipartimento di Scienze della Terra, Università degli Studi di Milano, via Mangiagalli 34, I-20133, Milano, Italy

^e Université de Franche-Comté, CNRS, Chrono-environnement, F-25000 Besançon, France

^f Dipartimento di Scienze Biologiche, Geologiche e Ambientali, Via Zamboni, 67, Bologna, Italy

^g Institut de Minéralogie, de Physique des Matériaux et de Cosmochimie (IMPIC), Sorbonne Université, Muséum National d'Histoire Naturelle, UMR CNRS 7590, IRD UR206, 75005 Paris, France

^h Institute of Geosciences and Earth Resources, National Research Council of Italy, Pisa, Italy

ARTICLE INFO

Keywords:

Carbon
Isotopes
COH-Fluid
Modeling
Thermodynamics

ABSTRACT

Carbon-bearing fluids and condensed carbon are common on and inside planetary bodies. Understanding the mechanisms capable of transferring carbon from fluids into solids and vice-versa is central in many fundamental and applied research targets within the Earth and Planetary Sciences. A broad range of applications can benefit from the thermodynamic properties of carbon-oxygen-hydrogen (COH) systems. As an example, the precipitation of natural graphite or diamond can be modeled within the COH thermodynamic systems. Because the evolution of COH fluids implies isotopic fractionation among different species, carbon stable isotopes can be used in conjunction with thermodynamic calculations to reconstruct graphite or diamond formation mechanisms, or the evolution of fluid species such as carbon dioxide or methane.

Thermotopes-COH is a Python-based graphical user interface (GUI) software for computation of thermodynamic and carbon isotopic modeling in the C–O–H system within the 0.1–5 GPa and 300–900 °C range. The software allows generic and process-oriented thermodynamic and carbon stable isotope calculations including fluid mixing, fluid-graphite/diamond interactions with changing pressure or temperature, and fluid desiccation. This versatile numerical tool is designed to model processes of dissolution/precipitation of graphite or diamond. Along with a description of the software functions, this contribution also provides practical examples.

1. Introduction

Carbon cycling on Earth is pivotal in bridging biological and geological processes, energy fluxes in both shallow and deep environments, and climatic and global environmental changes (Berner, 1999; Dasgupta, 2013; Dasgupta and Hirschmann, 2010; Evans, 2011). Carbon is ubiquitous in geologic fluids, e.g., in hydrocarbon-rich fluids, as small fractions in aqueous fluids or dominant in CO₂-rich systems (Connolly and Cesare, 1993; Huang et al., 2017; Kokh et al., 2017). Carbon isotope geochemistry has long been used to track sources and processes in geologic systems (Baumgartner and Valley, 2001; Bebout and Fogel,

1992; Duke and Rumble, 1986; Kitchen and Valley, 1995; Luque et al., 2012; Mason et al., 2017; Ray, 2009; Ray and Ramesh, 2000; Stachel et al., 2017; Tumiatì et al., 2022; Valley, 1986).

Carbon also is a redox-sensitive element, and its isotopic evolution strongly depends on the thermodynamic evolution of the geologic system under consideration. The COH thermodynamic system has long been used to model the evolution of many geological fluids and fluid-rock systems as a function of pressure (P), temperature (T), and redox state. Some examples include the study of graphite or diamond precipitation from carbon-saturated/supersaturated fluids, graphite dissolution in response to regional metamorphism or fluid infiltration, and the

* Corresponding author. Dipartimento di Scienze della Terra, Università degli Studi di Torino, Via Valperga Caluso 35, 10100 Torino, Italy.

** Corresponding author. Dipartimento di Scienze Biologiche, Geologiche e Ambientali, Via Zamboni, 67, Bologna, Italy.

E-mail addresses: antoine.boutier@unito.it (A. Boutier), alberto.vitaleb@unibo.it (A. Vitale Brovarone).

subsequent speciation in fluid inclusions (Cesare, 1995; Connolly, 1995; Connolly and Cesare, 1993; French, 1966; Ohmoto and Kerrick, 1977; Taylor and Liou, 1978; Taylor and Green, 1986; Ulmer and Luth, 1991; Huizenga 2005; Galvez et al., 2013; Vitale Brovarone et al., 2020).

The thermodynamics of the COH system has also been used to reconstruct the carbon isotopic evolution of graphite or diamond precipitation at carbon saturation conditions (Duke and Rumble, 1986; Stachel et al., 2017; Ortega et al., 2010; Boutier et al., 2023). While the relations governing the chemical equilibria of the COH system and its isotopes exist (Duke and Rumble, 1986; Holloway, 1984; Huizenga, 2005; Spycher and Reed, 1988; Rumble and Hoering, 1986), their integration into a single, user-friendly software is not yet available. Furthermore, when complex fluid or fluid/rock evolutions are considered within the COH system, the isotopic trend of the resulting fluid and solid phases may be challenging to model or even counterintuitive (Stachel et al., 2017).

Although numerical tools allowing computation of simple isotope equilibria exist (e.g., Beaudoin and Therrien, 2009, 2004), the computations are often done using user-made, specific spreadsheets. The Thermotopes-COH software integrates carbon isotope and thermodynamic models allowing for complex fluid and fluid-rock reactions and interactions within the COH chemical system. It features multiple functions through five interactive tabs: (1) carbon isotopic equilibrium, (2) carbon isotopic fractionation modeling, (3) multi-component solid-C precipitation, (4) COH fluid speciation, and (5) graphite/diamond dissolution/precipitation. The core of Thermotopes-COH provides advanced tools to model the thermodynamic and isotopic evolution of fluids and their interactions with graphite/diamond-bearing rocks within the COH chemical system. The software offers generic and process-oriented modeling options spanning the most common mechanisms of graphite/diamond precipitation or dissolution and a fast graphical visualization of the modeling results. The software also offers the possibility to perform conventional calculations such as carbon isotopic equilibria and fractionation modeling for further use as internal input parameters for the more advanced options.

This Python-based software runs on Windows and MacOS. It is a standalone executable that does not require any additional installation of packages. The software and documentation are available at <https://zenodo.org/records/10361692>. This contribution presents the software functions and principles, as well as examples of applications of its functionalities.

2. Isotope and thermodynamic database

2.1. Isotope database

Isotope fractionation equations can be presented under various form, with the most comprehensive as follow:

$$\Delta = 1000 \ln \alpha = A \frac{(10^{3n})}{T^n} + \dots + D \frac{(10^6)}{T^2} + E \frac{(10^3)}{T} + F \quad (1)$$

where Δ is the isotopic fractionation, α is the fractionation factor, A to F are experimentally determined parameters and T is temperature in K.

Since the higher order terms have been recognized to contribute insignificantly to isotopic fractionation between two phases (Richet et al., 1977), the isotopic database of Thermotopes-COH uses a simplified version of the general equation limited to the second power:

$$\Delta = 1000 \ln \alpha = A \frac{(10^6)}{T^2} + B \frac{(10^3)}{T} + C \quad (2)$$

This model includes a wide range of available references in the COH system but may limit the implementation of additional fractionation factors containing higher order terms. The full list of fractionation factors featured in the carbon isotopic database used in Thermotopes-COH is presented in Table 1.

Table 1

List of fractionation factor available in Thermotopes-COH.

Isotopic Couple	Temperature range	Reference
CO ₂ -CH ₄	0–700 °C	Bottinga (1969)
Graphite-CH ₄	0–700 °C	Bottinga (1969)
Calcite-CH ₄	0–700 °C	Bottinga (1969)
Calcite-Aragonite	25 °C	Rubinson and Clayton (1969)
Diamond-Graphite	0–1000 °C	Bottinga (1969)
Calcite-CO ₂	100–700 °C	Bottinga (1969)
Calcite-Graphite	0–100 °C	Deines et al. (1974)
	900 °C	Rosenbaum (1994)
	0–600 °C	Ohmoto and Rye (1979)
	0–700 °C	Bottinga (1969)
	400–800 °C	Dunn and Valley (1992)
	400–680 °C	Wada and Suzuki (1983)
	600–1200 °C	Scheele and Hoefs (1992)
	700–800 °C	Kitchen and Valley (1995)
CO ₂ -Graphite	600–1400 °C	Deines and Eggler (2009)
	100–700 °C	Bottinga (1969)
	0–1000 °C	Bottinga (1969)
	0–1000 °C	Bottinga (1969)
Diamond-CO ₂		Bottinga (1969)
Diamond-CH ₄		Bottinga (1969)
Dolomite-CO ₂		Ohmoto and Rye (1979)
Calcite-HCO ₃	0–100 °C	Deines et al. (1974)
CO-CO ₂	0–330 °C	Ohmoto and Rye (1979)

2.2. Thermodynamic database

The thermodynamic calculations in the Thermotopes-COH software follow the COH model by Huizenga (2005) based on the numerous equations of state available allowing a wide range of initial input parameters. The thermodynamic data for solids are taken from Shi and Saxena (1992). The list of considered oxygen fugacity buffers is presented in Table 2. The thermodynamic dataset for diamond/graphite is from Day (2012).

3. Thermotopes-COH structure and functions

This section presents the modeling functions of Thermotopes-COH, their assumptions, and some practical examples. The Thermotopes-COH GUI displays five different tabs. The first three tabs are designed to obtain input parameters for the following ones. The tabs called “Isotopic equilibrium” and “Isotopic fractionation”, respectively, provide isotopic input parameters at desired conditions, including simple isotope equilibria and open/closed system isotope fractionation. The third tab, called “Multicomponent solid-C” provides a first coupling of COH thermodynamics and isotope evolution for multi-component, carbon-saturated systems. The fourth tab, called “COH system” is centered on the thermodynamics of the COH system and provides carbon isotope evolution for fluid and solid species. The fifth tab, called “Dissolution/precipitation”, provides process-oriented integration of thermodynamic and isotope evolutions of fluid species and condensed carbon minerals (graphite/diamond).

Table 2

List of oxygen fugacity buffers available in Thermotopes-COH.

Oxygen fugacity buffer	Reference
FMQ (<i>Fayalite-Magnetite-Quartz</i>)	Miozzi and Tumiati (2020) O'Neill (1987) and Ballhaus et al. (1991) Ohmoto and Kerrick (1977)
Hem-Mag (<i>Hematite-Magnetite</i>)	Ballhaus et al. (1991) Frost (2018)
Fe-Wus (<i>Iron-Wustite</i>)	Ballhaus et al. (1991) Frost (2018)
Ni-NiO	Ballhaus et al. (1991) Frost (2018)
EMOD (<i>Enstatite-Magnesite-Olivine-Diamond/Graphite</i>)	Stagno and Frost (2010)

3.1. Isotopic equilibrium

The tab labeled “Isotopic equilibrium” is the basic building block of Thermotopes-COH. It calculates isotopic equilibrium between two carbon-bearing species, using the following expression:

$$\delta_A = \delta_B + \Delta_{A-B} \quad (3)$$

where δ_A is the isotopic composition of A in per mille (‰), δ_B is the isotopic composition of B in permil (‰), Δ_{A-B} is the isotopic shift between A and B calculated after Eq. (2) (Kendall and McDonnell, 2012; Sharp, 2017). The list of isotopic couples available in this tab is shown in Table 1.

3.2. Isotopic fractionation

The tab labeled “Isotopic fractionation” calculates batch or Rayleigh fractionation evolutions of a C-bearing species. Isotopic fractionation between species A to B is calculated at equilibrium. Batch (or closed system) fractionation is derived from mass balance equation (Valley, 1986):

$$\delta_B^f = (\delta_A^{initial} - \Delta_{A-B}) \times (1 - f) + (\delta_A^{initial} \times f) \quad (4)$$

$$\delta_A^f = \delta_B^f + \Delta_{A-B} \quad (5)$$

Rayleigh (or open system) fractionation follows the so-called

Rayleigh equation (Rayleigh, 1896):

$$\delta_A^f = ((1000 + \delta_A^{initial})f^{\alpha_{A-B}-1}) - 1000 \quad (6)$$

$$\delta_B^f = \frac{(1000 + \delta_A^f)}{\alpha_{A-B}} - 1000 \quad (7)$$

where f is the remaining fraction of A, $\delta_A^{initial}$ is the initial isotopic composition at the beginning of the fractionation, δ_A^f and δ_B^f are the isotopic composition at f , and α_{A-B} is the fractionation factor calculated after Eq. (2) (Dansgaard, 1964; Kendall and McDonnell, 2012; Sharp, 2017; Valley, 1986).

Fig. 1 shows two examples of modeling outputs for the isotope fractionation of graphite to either CO₂ or CH₄ in closed or open system conditions, at 300 °C and 500 °C. This example provides a quick visualization of the effect of temperature on the fractionation factor of the graphite-CO₂ and graphite-CH₄ couples. It shows, for example, that the temperature effect is more important for the graphite-CH₄ couple. This behavior has an important role in the isotopic evolution of multi-component systems described in the next section.

3.3. Multi-component graphite/diamond-CO₂-CH₄ modeling

The tab labeled “Multi-component solid-C” models the precipitation of either graphite or diamond, from a fluid containing both CO₂ and CH₄ according to the equation described successively by Ray (2009), Ray and

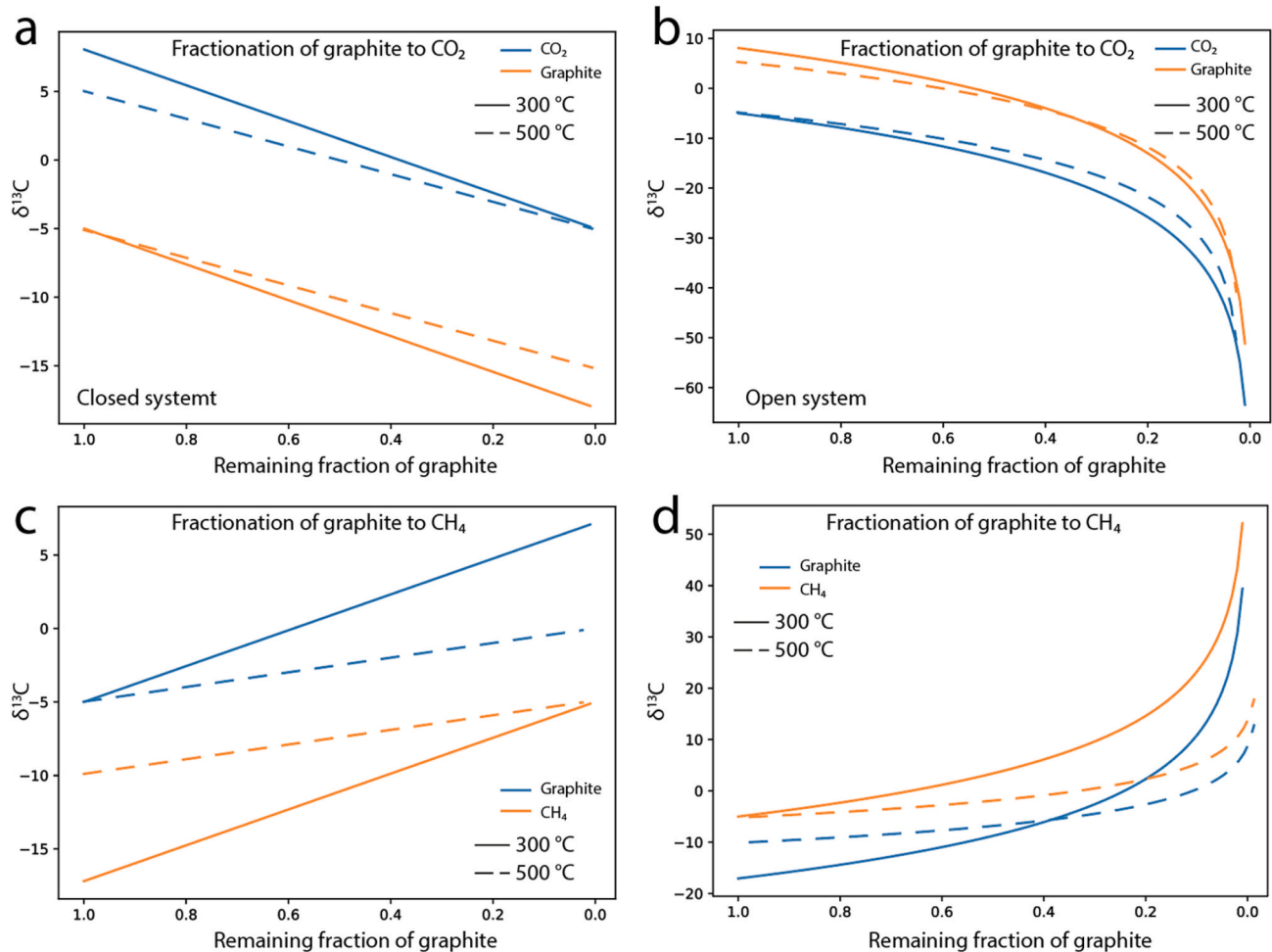


Fig. 1. Examples of closed (a, c) and open (b, d) system fractionation of graphite to either CO₂ (a, b) or CH₄ (c, d). Each panel shows fractionation evolution at 300 (solid line) and 500 °C (dashed line), respectively. The software allows to easily select a source and a product and to model their isotopic evolution as a function of the remaining fraction of the source at a given temperature. All species and fractionation factor available in the software are given in Table 1.

Ramesh (2000), and by Stachel et al. (2017). The precipitation of graphite/diamond from a fluid containing both CO₂ and CH₄ follows two steps: initially, and as long as available, CO₂ and CH₄ contribute equally to the isotopic value of the resulting C_{solid} (0.5 mol each per mole of produced graphite/diamond). Then, when the less abundant phase either CH₄ or CO₂ is totally consumed, precipitation evolves as a single component system following a classical Rayleigh model (see Table 2). During the first step, Eqs. (12) and (17) defining the isotopic value of C_{solid} varies if the system is CH₄ or CO₂ dominated (Ray, 2009; Ray and Ramesh, 2000; Stachel et al., 2017b). When CH₄ is more abundant than CO₂ the equations are:

$$\delta^{13}C_{fluid}^f = 1000 \left(\frac{\alpha_{C-CH_4}}{A} \ln \frac{Af - B}{A - B} - \ln f \right) + \delta^{13}C_{fluid}^{initial} \quad (8)$$

$$\delta^{13}C_{C\ solid}^f = 1000 \left(\frac{\alpha_{C-CH_4}}{A - \frac{B}{f}} - 1 \right) + \delta^{13}C_{fluid}^f \left(\frac{\alpha_{C-CH_4}}{A - \frac{B}{f}} \right) \quad (9)$$

$$r = \frac{XC_{CO_2}}{XCH_4} \quad (10)$$

$$A = \frac{1 + \alpha_{CO_2-CH_4}}{2} \quad (11)$$

$$B = (1 - r) \frac{\alpha_{CO_2-CH_4} - 1}{2 + 2r} \quad (12)$$

When CO₂ is more abundant than CH₄:

$$\delta^{13}C_{fluid}^f = 1000 \left(\frac{\alpha_{C-CO_2}}{A} \ln \frac{Af - B}{A - B} - \ln f \right) + \delta^{13}C_{fluid}^{initial} \quad (13)$$

$$\delta^{13}C_{C\ solid}^f = 1000 \left(\frac{\alpha_{C-CO_2}}{A - \frac{B}{f}} - 1 \right) + \delta^{13}C_{fluid}^f \left(\frac{\alpha_{C-CO_2}}{A - \frac{B}{f}} \right) \quad (14)$$

$$r = \frac{XCH_4}{XCO_2} \quad (15)$$

$$A = \frac{1 + \frac{1}{\alpha_{CO_2-CH_4}}}{2} \quad (16)$$

$$B = (1 - r) \frac{\alpha_{CO_2-CH_4}}{2 + 2r} \quad (17)$$

where $\delta^{13}C_{fluid}^{initial}$ is the initial isotopic composition of the fluid, $\delta^{13}C_{fluid}^f$ the isotopic composition of the fluid for a remaining fraction of fluid f , $\delta^{13}C_{C\ solid}^f$ is the composition of graphite/diamond at the remaining fraction of fluid f , $\alpha_{CO_2-CH_4}$ the fractionation factor between CO₂ and CH₄, α_{C-CO_2} the fractionation factor between graphite/diamond and CO₂ and α_{C-CH_4} the fractionation factor between graphite/diamond and CH₄.

Multi-component isotope calculations are performed by selecting an option for the input of $\delta^{13}C$ isotopic composition of the fluid, either "Total C", "Fluid mixing", "Known CH₄ composition" or "Known CO₂ composition".

- Total C: The fluid is considered in internal isotopic equilibrium and the total $\delta^{13}C$ value of the fluid is entered. The isotopic compositions of CO₂ and CH₄ are then calculated based on their respective proportion at the desired temperature.
- Fluid mixing: Two fluids initially at isotopic disequilibrium contain either CO₂ or CH₄. Once the precipitation starts, the two fluids mix to reach isotopic equilibrium and then ensue the precipitation of graphite/diamond.

- Known CH₄ (or CO₂) composition: The fluid is at isotopic equilibrium but only the $\delta^{13}C$ CH₄ (or CO₂) composition is known by the user. In this case, the software will model the associated missing $\delta^{13}C$ composition at the desired temperature and derives the precipitation of graphite/diamond.

Please note that the modeling of graphite/diamond precipitation from the tab "Multi-component G/D-C-O-H modeling" does not involve thermodynamic computations. Nevertheless, the isotopic mass balance used for the multi-component modeling follows the same principles of evolving COH speciation as those that define the thermodynamic modeling presented in section 3.4.

Fig. 2 shows two examples of multi-component graphite precipitation models for CH₄/CO₂ ratios >1 and <1, respectively, at 300 °C and 500 °C. The initial bulk $\delta^{13}C$ is -5‰ in both cases. The evolution of single component systems for either CH₄ or pure CO₂ is also shown for comparison. As observed by Stachel et al. (2017), the evolution of multi-component systems may result in counterintuitive trends. In Fig. 2, it can be observed that, depending on the initial CH₄/CO₂ ratio, the coexisting fluid and graphite follow consistent (CH₄/CO₂ ratio <1) or opposite trends (CH₄/CO₂ ratio >1), because $\Delta_{\text{graphite-CH}_4}$ is smaller than $\Delta_{\text{graphite-CO}_2}$. This results in a progressive enrichment in ¹³C in the precipitating graphite and a progressive enrichment in X_{CH₄} (and therefore a depletion in ¹³C in the remaining fluid) for fluid with CH₄/CO₂ ratio >1, or a progressive enrichment in both ¹³C in the precipitating graphite and X_{CO₂} for fluid with CH₄/CO₂ ratio <1. Depending on the temperature conditions, the fluid and graphite isotopic trends do or do not cross each other (Fig. 2). This is the result of the multi-component evolution, when the fluid and precipitating solid may transiently have the same $\delta^{13}C$ composition. Such a feature is generally observed for a complete transformation in a closed reservoir (for example, full transformation of CO₂ to graphite), whereas in the present case it is observed for transient open-system conditions. As introduced in the previous section, the diversity in temperature dependence between the graphite-CO₂ and graphite-CH₄ couples determines remarkable variations in the isotopic fractionation of the precipitating graphite, especially for CH₄/CO₂ ratios >1. In particular, at 300 °C for a CH₄/CO₂ ratio >1, the first precipitating graphite is enriched in ¹³C relative to the fluid source, whereas at 500 °C the first precipitating graphite is depleted in ¹³C relative to the fluid source. This is due to the difference between $\Delta_{\text{graphite-CH}_4}$ and $\Delta_{\text{graphite-CO}_2}$ that decreases with increasing temperature. In other words, $\Delta_{\text{CH}_4\text{-CO}_2}$ decreases with increasing temperature but with more substantial variations for the CH₄-graphite pair. Although $\Delta_{\text{graphite-CH}_4}$ remains smaller than $\Delta_{\text{graphite-CO}_2}$ with increasing temperature, the decreasing $\Delta_{\text{CH}_4\text{-CO}_2}$ with increasing temperature determines, for a fixed CH₄/CO₂ ratio >1, that the first precipitating graphite is enriched in ¹³C relative to the fluid source at low temperature, whereas it is depleted in ¹³C relative to the fluid source at higher temperature. The successive fractionation trends are controlled by the evolving CH₄/CO₂ ratio as described above.

3.4. COH fluid speciation

The tab labeled "COH system" models the speciation of COH fluids, the carbon activity, the X_O, and the oxygen and hydrogen fugacities. The modeling follows equations from Huizenga (2005) and references therein, and calculates the speciation of the COH fluid using the following equilibria:



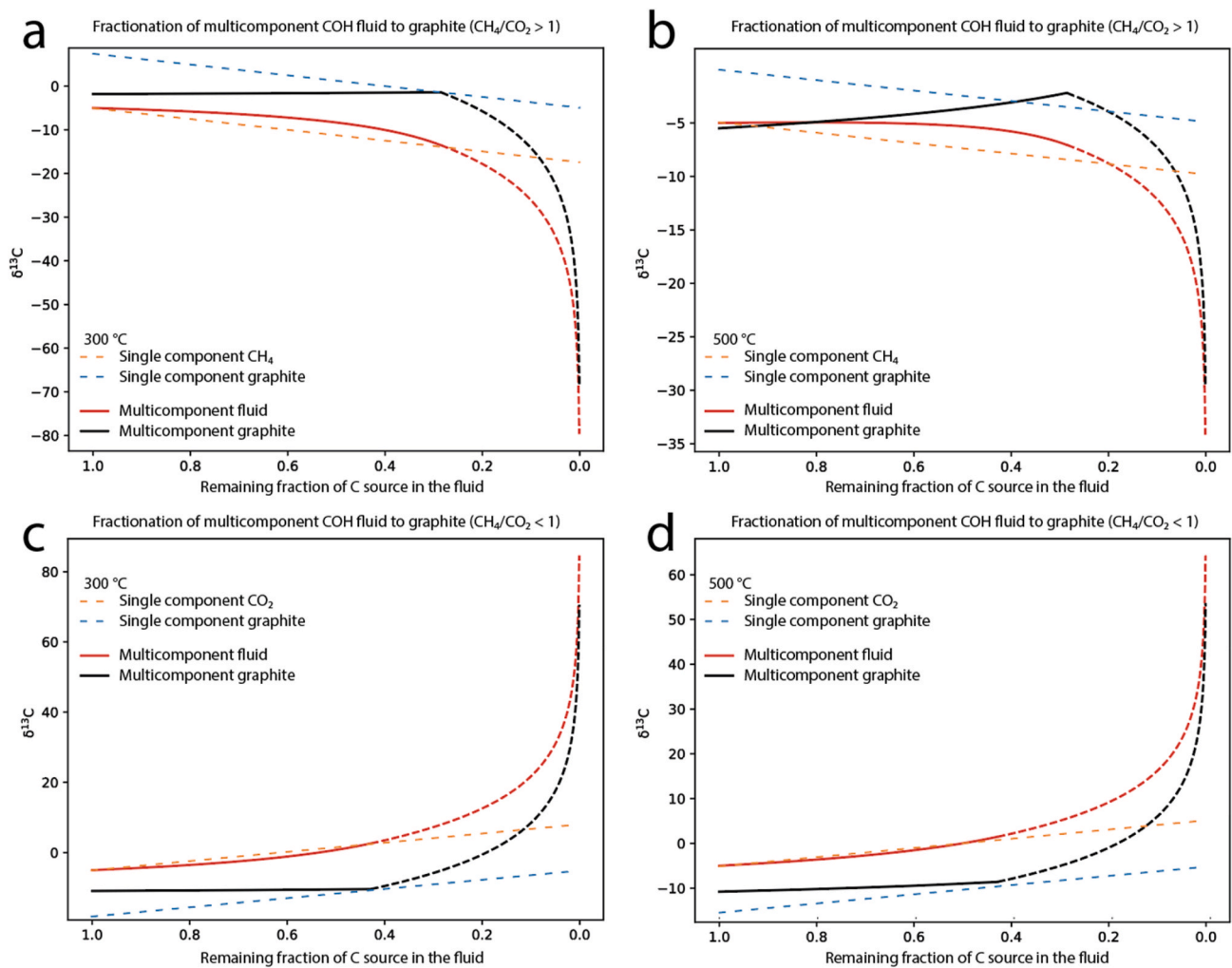


Fig. 2. Examples of multi-component isotope fractionation trends for $\text{CH}_4/\text{CO}_2 = 1.8$ (CH_4 0.64; CO_2 0.36) at 300 °C (a) and 500 °C (b) and $\text{CH}_4/\text{CO}_2 = 0.4$ (CH_4 0.29; CO_2 0.71) at 300 °C (c) and 500 °C (d), for initial $\delta^{13}\text{C} = -5$ ‰. Single component fractionations are also shown for reference. The system firstly evolves as multi-component (solid lines) until the less abundant molecule – CO_2 in (a,b), CH_4 in (c,d)– is exhausted. Secondly, it evolves as a single-component system (dashed lines).



From these equilibria, the oxygen fugacity f_{O_2} along with the molar fractions of $X_{\text{H}_2\text{O}}$, X_{CO_2} , X_{CH_4} , X_{H_2} and X_{CO} , are calculated. X_{O} is defined as $X_{\text{O}} = \frac{n_{\text{O}}}{n_{\text{O}} + n_{\text{H}}}$ where n_{O} and n_{H} are the atomic proportions of oxygen and hydrogen in the fluid, respectively (Connolly and Cesare, 1993).

The model assumes ideal mixing. Details of the equation for the equilibrium constants of reaction and fugacity coefficients can be found in Huizenga (2005) and reference therein.

f_{H_2} is calculated according to the following equation (Holloway, 1977):

$$f_{\text{H}_2} = \gamma_{\text{H}_2} \times P \times X_{\text{H}_2} \quad (22)$$

Where X_{H_2} is the molar fraction of H_2 , P is the pressure in bar, and γ_{H_2} is the fugacity coefficient of hydrogen calculated following Huizenga (2005). The carbon activity is the effective concentration of carbon in the fluid. A carbon activity of 1 indicates that the fluid is saturated in carbon and coexists with graphite/diamond. Carbon activity above to 1 refers to a carbon oversaturated fluid or to the equilibrium with a non-ideal (e.g., disordered) carbon form (Tumiati et al., 2020; Vitale Brovarone et al., 2020), which is not integrated in the current version of the software. Carbon activity lower than one refers to graphite/diamond-undersaturated conditions.

Several modeling options are available that require either 2 or 3 input parameters among:

- known carbon activity, f_{O_2} buffer, and a $\Delta \log f_{\text{O}_2}$ from this buffer
- known carbon activity and $X_{\text{CO}_2}/(X_{\text{CO}_2} + X_{\text{CH}_4})$ ratio. A f_{O_2} buffer can be indicated for reference.
- known $X_{\text{CO}_2}/(X_{\text{CO}_2} + X_{\text{CH}_4})$ ratio, f_{O_2} buffer, and a $\Delta \log f_{\text{O}_2}$ from this buffer
- known carbon activity and X_{O} . A f_{O_2} buffer can be indicated for reference.
- known $X_{\text{CO}_2}/(X_{\text{CO}_2} + X_{\text{CH}_4})$ ratio and XH_2O . A f_{O_2} buffer can be indicated for reference.

The $\Delta \log f_{\text{O}_2}$ correspond to the relative difference to the selected oxygen fugacity buffer. For example, for a fluid at $\Delta \text{FMQ}+1$ (log units), $\Delta \log f_{\text{O}_2}$ value is 1.

The results can be visualized on a ternary COH diagram (Fig. 3). The latter displays the location of the carbon saturation curve and the position of the modeled COH fluid composition. The software also allows expanding the computations over a pressure-temperature range and to plot them on a P-T diagram (Fig. 4).

3.4.1. Application to the study of carbon-saturated fluid inclusions

A potential application of the COH system tab is for the post

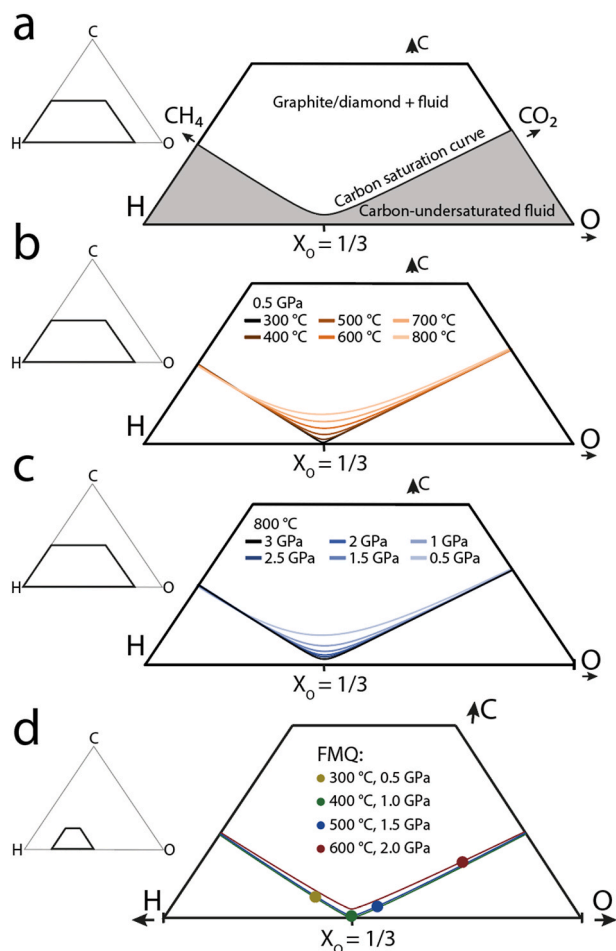


Fig. 3. (a) Example of ternary COH diagram showing a generic carbon saturation curve separating the field of carbon-undersaturated fluids from the field where the fluid coexists with graphite/diamond. (b–d) Ternary COH diagrams showing the position of the carbon saturation curve for different temperatures and constant pressure (b), for different pressures at constant temperature (c), and along a prograde metamorphic path highlighting the positions of the FMQ buffer for four pressure-temperatures couples (d). FMQ buffer from Miozzi and Tumiati (2020).

entrapment fluid-component re-speciation in carbon-saturated fluid inclusions. Cesare (1995) described the transformation of graphite-saturated fluid inclusions during cooling and decompression. Provided that no mass is gained or lost by the inclusions, the original X_O ratio of the fluid phase should be constant (Cesare, 1995). Because the position of the carbon saturation curve within the COH diagram is dependent upon P and T conditions, cooling and/or decompression drive variations in fO_2 and carbon content of the fluid, which in turn leads to the precipitation of graphite inside the inclusions. As a consequence, carbon speciation changes inside the fluid phase of the inclusions. By compiling results for a series of P-T couples, Cesare (1995) concluded that the $CO_2/(CO_2 + CH_4)$ ratio increases during cooling for fluids with initial $XO > 1/3$, whereas it decreases for fluids with initial $XO < 1/3$. The P-T graph option of the COH system tab of Thermotopes-COH offers the possibility to plot the $CO_2/(CO_2 + CH_4)$ ratio of graphite-saturated fluids for constant X_O values and to assess the carbon speciation in the fluid along any cooling and decompression path (Fig. 5). The fO_2 variation can also be plotted. If a fixed composition for the initial graphite in equilibrium with the trapped fluid is set, the software allows the calculation of P-T diagrams of $\delta^{13}C$ values for the bulk fluid, CH_4 , or CO_2 . Since these diagrams assume a constant isotopic value for the graphite in equilibrium with the fluid inclusion, the $\delta^{13}C$

values across a P-T diagram generated through the COH tab do not take into account any isotopic mass balance during the precipitation of graphite inside the inclusions with decreasing pressure and temperature, which would induce isotopic fractionation of the remaining fluid. For this reason, it is not recommended to use boldly the $\delta^{13}C$ results of the COH tab to track the isotopic evolution of fluid inclusions during pressure and temperature variations unless the assumption is made that the solid carbon precipitated inside the inclusion does reequilibrate isotopically after its formation. A way to overcome this issue consists in considering a $\delta^{13}C$ equal to 0‰ for the graphite coexisting with the fluid. This way, the P-T diagrams for carbon isotopes represent directly the Δ between the fluid phases (bulk, CO_2 , or CH_4) and the solid inside the inclusion.

3.5. Dissolution/precipitation of graphite/diamond

The tab labeled “Dissolution/precipitation”, offers process-oriented solutions to investigate the precipitation and/or dissolution of graphite/diamond. The model assumes equilibrium conditions and tracks the carbon activity of a COH-fluid through various reactions according to the equations in Huizenga (2005). In short, graphite/diamond precipitation is obtained for any fluid evolution resulting in carbon activity higher than 1, or when a carbon-saturated fluid evolves along the carbon saturation curve from H_2O richer to H_2O poorer compositions. Graphite/diamond dissolution is observed when the fluid evolves from carbon-saturated conditions to carbon undersaturated conditions, or when a fluid evolves from H_2O poorer to H_2O richer compositions along the carbon saturation curve. The governing equilibrium is:



The respective isotopic composition of the solid and fluid is calculated along the reaction path according to reaction (23).

Since graphite/diamond may behave as a chemically reactive but isotopically inert phase (Tumiati et al., 2022; Valley and O’Neil, 1981), an option is provided to allow graphite/diamond to participate in the isotopic mass balance. When this option is toggled on, the initial and newly formed graphite/diamond in the system can freely equilibrate with other C-bearing species in the system and participate in the mass balance. The isotopic system is considered to be closed, with carbon being either in the fluid phase or as graphite/diamond. The composition of solid-C is calculated through the following equation:

$$\delta^{13}C_{solid} = \delta^{13}C_{system} - \frac{nCO_2}{nC_{total}} \Delta_{CO_2-C} - \frac{nCH_4}{nC_{total}} \Delta_{CH_4-C} \quad (24)$$

with $\delta^{13}C_{solid}$ being the isotopic composition of solid-C, $\delta^{13}C_{system}$ the isotopic composition of the system, nCO_2 and nCH_4 the number of moles of CO_2 and CH_4 , respectively, nC_{total} the total number of moles of carbon in the system Δ_{CO_2-C} and Δ_{CH_4-C} the isotopic capital delta between CO_2 and graphite/diamond and CH_4 and graphite/diamond, respectively.

When this option is toggled off, graphite/diamond in the system does not participate in the isotopic mass balance unless a fraction of this solid-C is dissolved. In this case, the isotopic composition of the newly formed graphite/diamond is calculated considering the instantaneous remaining fraction of carbon in the fluid f as follows:

$$f = 1 - \left(\frac{nC_{solid\ new}}{nC_{CH_4} + nC_{CO_2}} \right) \quad (25)$$

The isotopic compositions of the instantaneous graphite/diamond and the total graphite/diamond are then calculated from a combination of Eq. (4) and an isotopic mass balance. A comparison of the isotopic calculation between the multicomponent system and the Dissolution/precipitation model is presented in Supplementary material 1.

Thermotopes-COH offers six conceptual models for graphite/diamond dissolution/precipitation, which are presented hereafter.

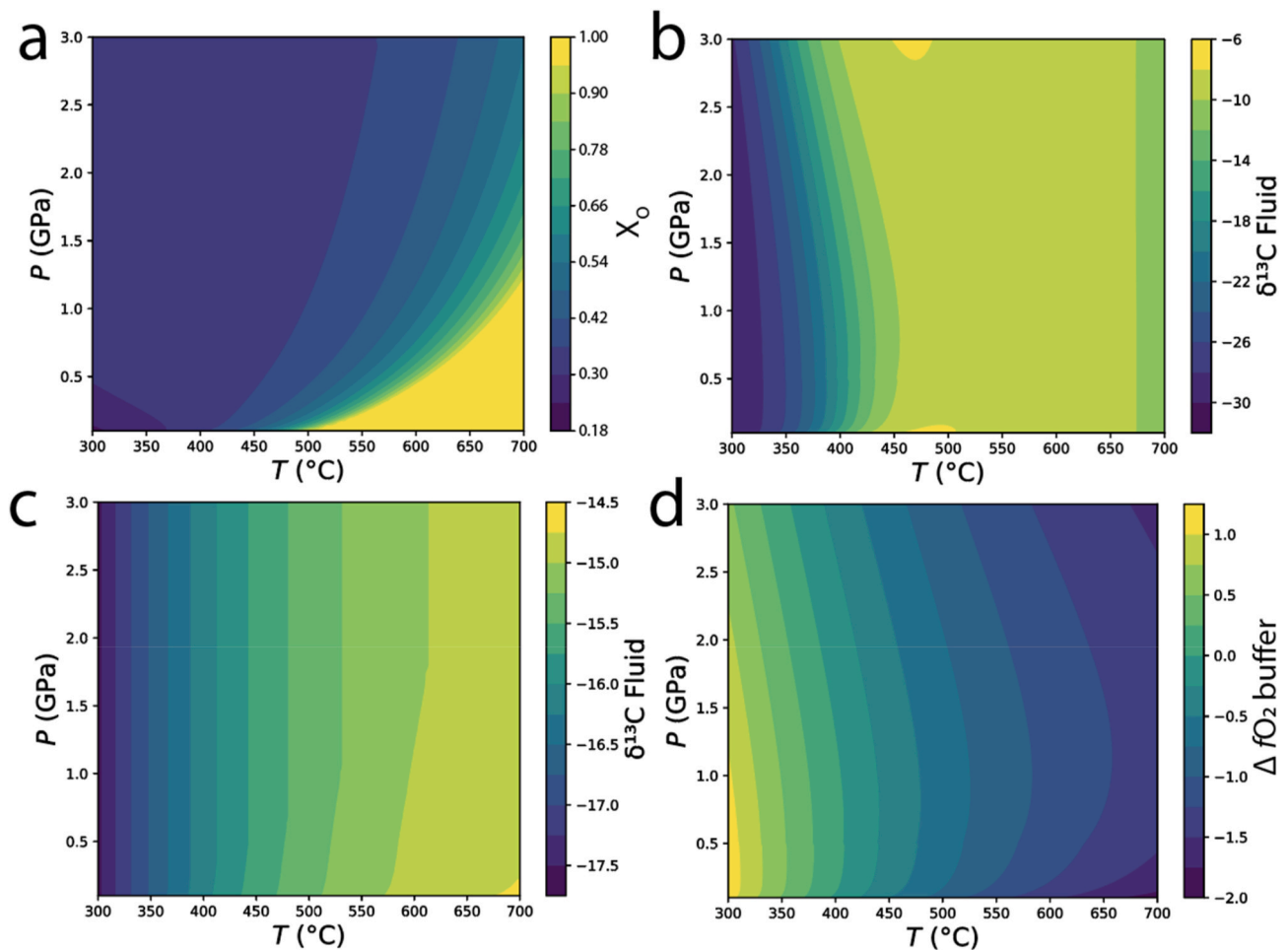


Fig. 4. (a) X_{O_2} colormap for a graphite saturated fluid at FMQ. (b) $\delta^{13}C$ colormap of a carbon-saturated fluid in equilibrium with graphite/diamond ($\delta^{13}C$ graphite = -18 ‰), at FMQ. (c) $\delta^{13}C$ colormap of a carbon-saturated fluid in equilibrium with graphite/diamond ($\delta^{13}C$ graphite = -18 ‰), at water-maximum conditions ($X_{O_2} = 1/3$). (d) $\Delta \log FMQ$ colormap for a carbon-saturated fluid at water maximum ($X_{O_2} = 1/3$).

3.5.1. Dissolution/precipitation of graphite/diamond during fluid mixing

The fluid mixing process models the interaction of two different COH-fluids and their resulting potential to dissolve or precipitate graphite/diamond. The software models the titration of the second fluid into the first one through an iterative process. The titration step is defined as 0.1% of the second fluid being mixed in the first one. The carbon activity of the fluid is calculated and, if $a_C = 1$, the titration proceeds to the next step. If the carbon activity is either >1 or <1 , a sub-iteration starts with either dissolution or precipitation of graphite/diamond until the carbon activity reaches 1. The associated isotopic evolution of fluid species and graphite/diamond is computed at each step. The titration proceeds until the totality of the second fluid is mixed within the first one.

Fig. 6 shows examples of models involving the mixing of 100 mol of reduced graphite-saturated fluid into 100 mol of a more oxidized one, at 500 °C and 1 GPa. The host fluid has a $CO_2/(CO_2 + CH_4)$ ratio of 0.95, corresponding f_{O_2} values equivalent to the FMQ buffer, and is in equilibrium with graphite with $\delta^{13}C = -30$ ‰, which corresponds to a $\delta^{13}C$ value of -20.6 for the fluid. The second fluid has a $CO_2/(CO_2 + CH_4)$ ratio of 1.9×10^{-4} , corresponding to $\Delta \log FMQ = -3$, and is in equilibrium with graphite with $\delta^{13}C$ of -5 ‰, which corresponds to a $\delta^{13}C$ of -34.9 ‰ for the fluid. Two examples are considered, with either inert or exchanging graphite in the host system (1 mol graphite), respectively. The amount of graphite precipitation, the f_{O_2} evolution, and the fluid component speciation are equivalent in both cases, and characterized by the precipitation of about 31 mol of graphite, a decrease of the f_{O_2} of

about 3 log units, and by an increase of the $CH_4/(CH_4 + CO_2)$ ratio from nearly 0 in the host fluid, to about 1 in the mixed fluid. The $\delta^{13}C$ of the system, however, is different in the two cases. The isotopic exchange of the host graphite (-30 ‰) results in a decrease of the $\delta^{13}C$ of CO_2 and increase of the $\delta^{13}C$ of CH_4 .

In these examples, it can be observed that the mixing of two carbon-saturated fluids may lead to transient, counterintuitive trends in the carbon isotope evolution of both the fluid species and the precipitated graphite. This includes isotopic values transiently heavier than the heaviest fluid being involved in the mixing. This effect is due to the evolution of the mixing in a complex multi-component ($CO_2 + CH_4$) system across the water-maximum: an initially CO_2 -dominated fractionation trend, followed by a CH_4 -dominated one, and a contextual precipitation of variable amounts of graphite during the mixing.

The software also offers the possibility to model fluid mixing at buffered f_{O_2} conditions. This option models the interaction of a fluid with an f_{O_2} buffer, to simulate interaction in a buffered medium. The f_{O_2} is $\Delta \log$ relative to a list of buffers (e.g., FMQ or EMOG), fixed during the whole process, and the software models the composition of an external fluid equilibrating with a constant f_{O_2} . If graphite/diamond precipitates, its isotopic composition is also calculated. Geologically, buffering the f_{O_2} is not a trivial assumption and should be selected only if consistent with the natural or experimental conditions.

3.5.2. Desiccation

This interaction models the evolution of a desiccating COH fluid (e.

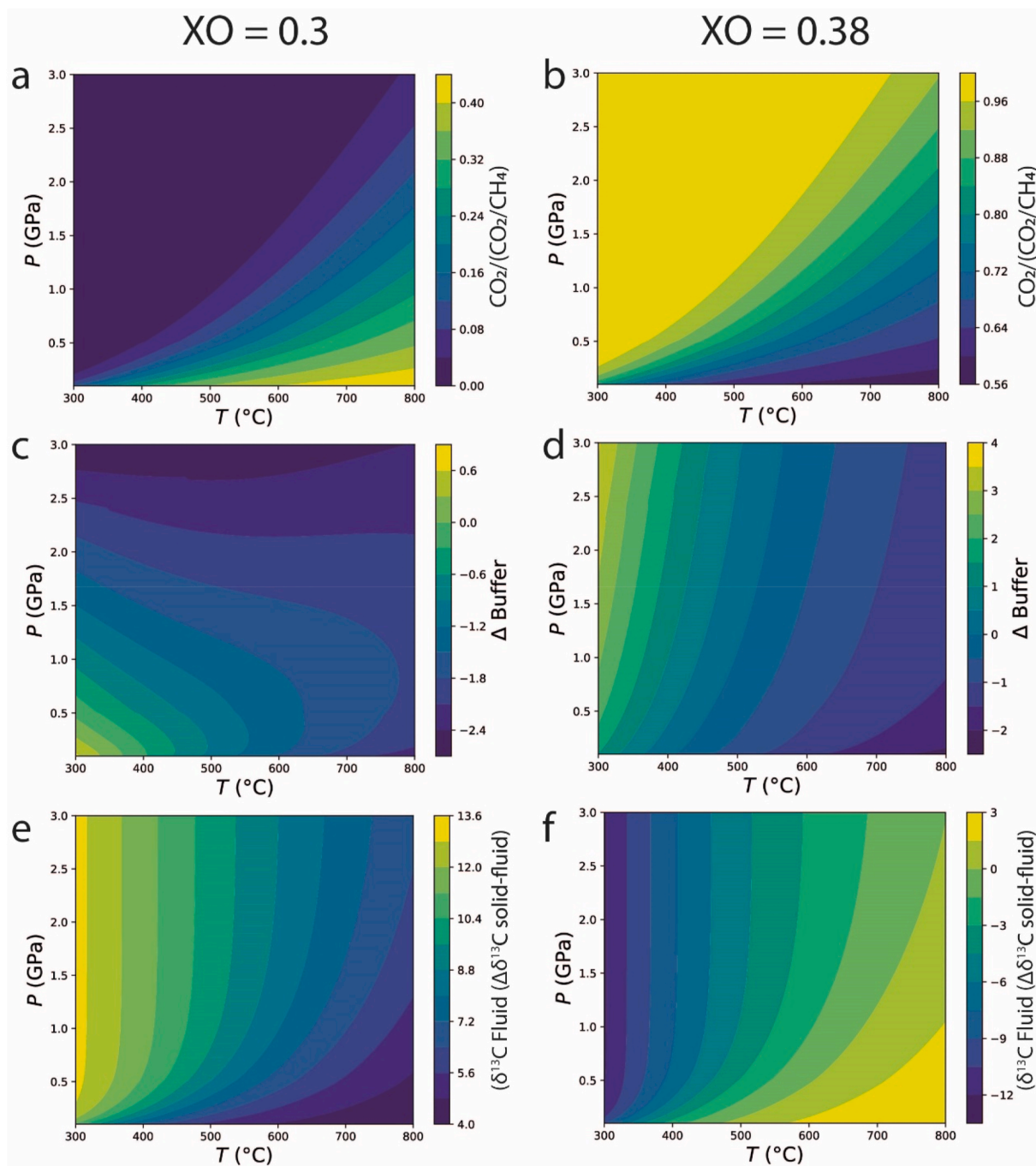


Fig. 5. Pressure-temperature diagrams for the carbon-saturated COH system. In (a) and (b), fixed X_{O} values of 0.3 and 0.38 are considered as representative of more reduced and more oxidized conditions, respectively, relative to the water-maximum conditions ($X_{\text{O}} = 1/3$). The ΔLogFMQ for both X_{O} values is also shown in (c) and (d), respectively. Panels (e) and (f) show the $\delta^{13}\text{C}$ evolution of the bulk fluid ($\text{CH}_4 + \text{CO}_2$). As explained in the text, these values across the P-T space refer to a constant $\delta^{13}\text{C}$ for the solid carbon in equilibrium with the fluid. These diagrams were constructed for a $\delta^{13}\text{C}$ value of solid carbon at 0‰, so that, at any point within the diagram, the $\delta^{13}\text{C}$ value directly refers to the $\Delta\delta^{13}\text{C}$ between the solid and the bulk fluid.

g., through rock hydration reaction, or respeciation of H and O into C-bearing fluid species) and calculates the associated precipitation of graphite/diamond. The desiccation is here defined as the loss of H_2O moles from the initial fluid. In the desiccation mode, the oxygen fugacity is free to evolve during the desiccation. During fluid desiccation, the carbon concentration increases and, if carbon saturation is reached, graphite/diamond precipitates. The degree of desiccation that is entered, corresponds to the fraction of the water loss ($X_{\text{H}_2\text{O}}$). The model is iterative and, at each step, 0.01% of the moles of the initial H_2O ($n\text{H}_2\text{O}$) is removed, the carbon activity is calculated, and the number of

moles of precipitated graphite/diamond and its isotopic value are derived. The calculation proceeds until the desired water fraction of the initial fluid is lost. Fig. 7 shows desiccation of a fluid slightly oxidized relative to the water maximum at 600 °C and 0.5 GPa ($\Delta\text{LogFMQ} = -0.5$, Fig. 7a). The $\delta^{13}\text{C}$ of the fluid was set at -10% , and the desiccation rate could proceed to 100%. Fig. 7b shows that, during the desiccation of the chosen carbon-saturated COH fluid, graphite is constantly precipitated during a progressive increase in f_{O_2} . Despite the desiccation ratio being set to 100%, the final fluid still contains some water (Fig. 7c). This water is produced in response to graphite/diamond precipitation

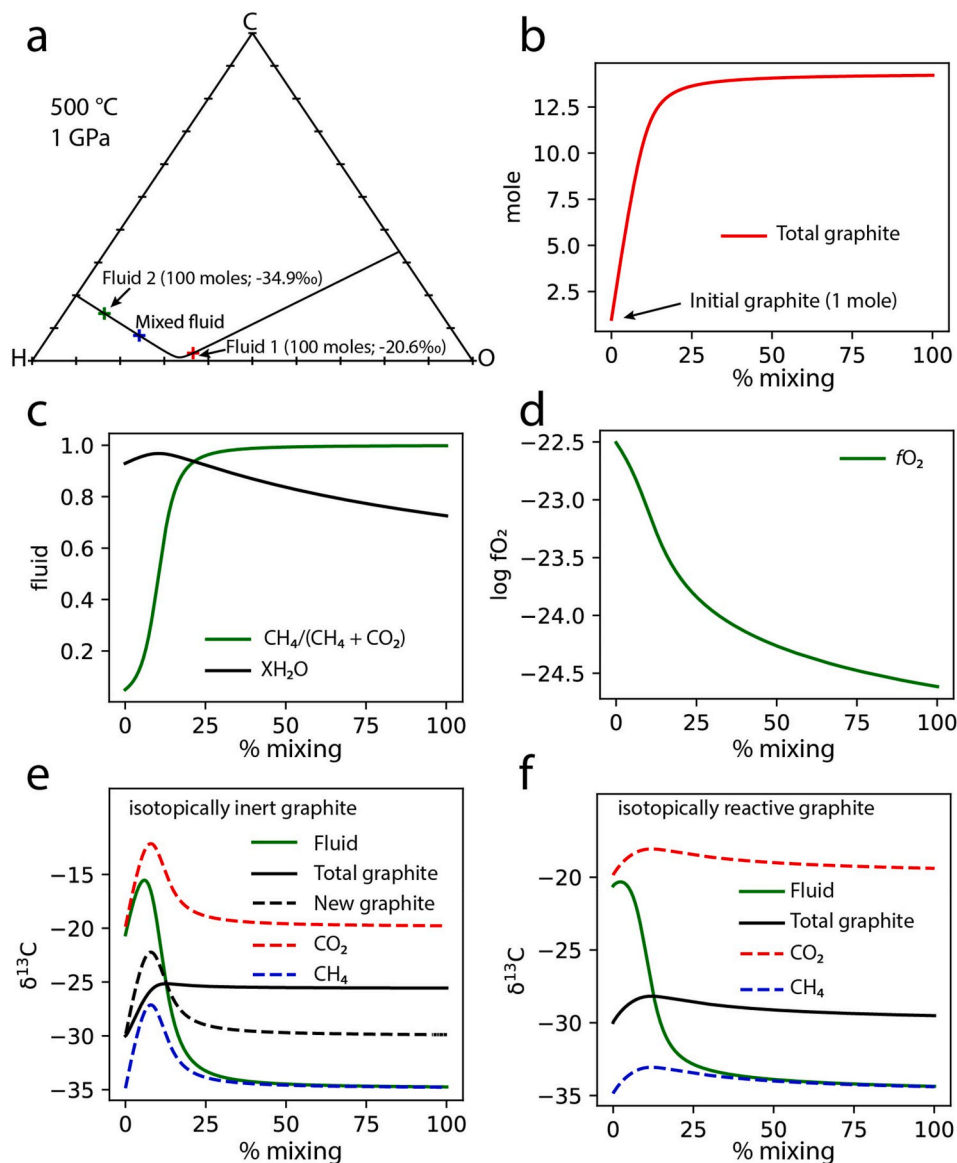


Fig. 6. Examples of graphite precipitation through fluid mixing. Panel (a) shows the position of the two mixing fluids (both carbon-saturated) and the final one. Panel (b) shows the number of moles of graphite precipitated due to mixing. Panel (c) shows the evolution of the $\text{CH}_4/(\text{CH}_4 + \text{CO}_2)$ ratio and XH_2O and (d) of the f_{O_2} during the mixing, respectively. Panels (e) and (f) show the $\delta^{13}\text{C}$ of the solid, the bulk fluid, CO_2 , and CH_4 during the mixing for isotopically inert (e) and isotopically exchanging (f) initial solid. The mixing of 100 mol of fluid 1 with 100 mol of fluid 2 was calculated at 500 °C, and for a preexisting graphite with $\delta^{13}\text{C} = -30\text{‰}$.

and is not accounted for by the desiccation process. The newly formed water remains in the fluid. At the chosen high temperature conditions, the $\delta^{13}\text{C}$ of the precipitating graphite shows minimal variations during the desiccation process. As introduced in the previous section, lower temperatures should increase the range of $\delta^{13}\text{C}$ values in an evolving carbon-saturated COH fluid.

Also, the desiccation option can be modeled at buffered f_{O_2} conditions. The desiccation is here defined as the loss of H_2O mole in the fluid, and because the f_{O_2} is fixed during the interaction, the water fraction in the fluid remains constant while the fluid stays at carbon saturation. In other words, the actual amount of water decreases rather than its molar fraction. Any loss of H_2O is accompanied by the loss of an equivalent amount of the other species in the fluid in order to maintain $X_{\text{H}_2\text{O}}$ constant. The amount of desiccation must be entered, because redox conditions are buffered, $X_{\text{H}_2\text{O}}$ remains constant during desiccation. If graphite/diamond precipitates, its isotopic composition is also calculated. Geologically speaking, buffering f_{O_2} is not a trivial assumption and this option should be used with caution. This option is probably better

suited to experimental rather than natural conditions.

3.5.3. Pressure change

The “pressure change” option models the evolution of a COH fluid at equilibrium undergoing isothermal pressure changes. The model is iterative. At each pressure step (every 0.01 GPa), the thermodynamic parameters of the COH system are calculated. If graphite/diamond is dissolved/precipitated, its isotopic composition is calculated.

3.5.4. Temperature change

The “temperature change” option models the evolution of an equilibrium COH fluid undergoing isobaric thermal changes. The model is iterative. At each temperature (every 1 °C), the thermodynamic parameters of the COH system are calculated. In the event of graphite/diamond is dissolved/precipitated, its isotopic composition is calculated.

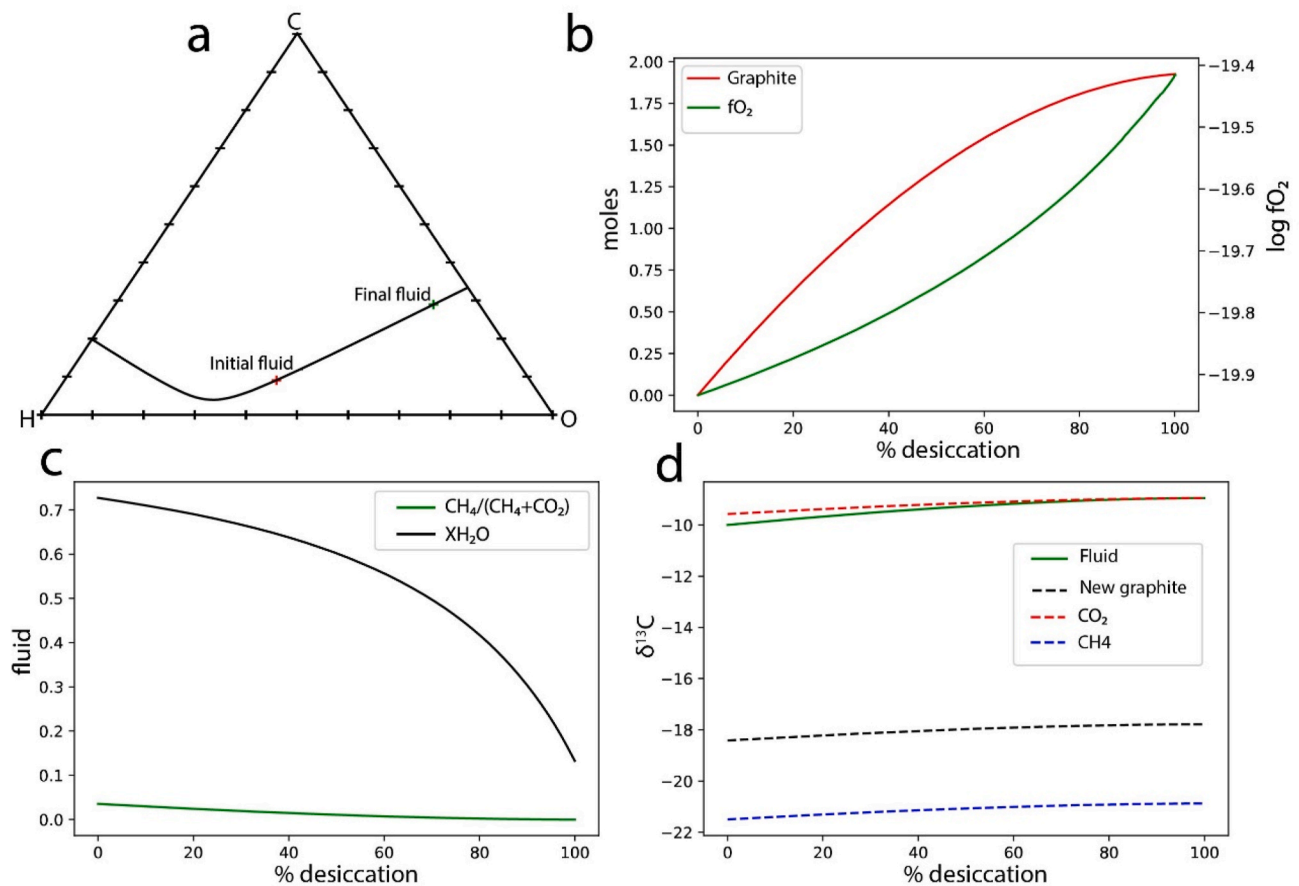


Fig. 7. Desiccation model at 600 °C and 0.5 GPa. The $\delta^{13}\text{C}$ of the fluid was set at -10% , and the $f\text{O}_2$ at $\Delta\text{LogFMQ} = -0.5$. Desiccation ratio was 100%. A: COH diagram showing the position of the fluid prior to the interaction and its final position after graphite precipitation. B: Evolution of graphite precipitation in response to changing $f\text{O}_2$ during desiccation. C: H_2O and $\text{CH}_4/(\text{CH}_4 + \text{CO}_2)$ proportions during desiccation. D: Isotopic composition of the fluid, of its C-bearing species CO_2 and CH_4 , and of graphite formed in response to fluid desiccation.

4. Limitations

4.1. Maximum temperature and pressure

The equation of state Thermotopes-COH software limits the applicable pressure-temperature range to crustal and upper mantle geological conditions and may react poorly in eclogitic or granulitic conditions. Thermodynamic equations from Huizenga (2005) cover the range above 300 °C and 0.1 GPa. Pairs of P-T values in proximity of the extremes of the allowed range may lead to unexpected results or errors.

4.2. Pure CO_2 or CH_4 fluid

At temperatures higher than ≈ 850 °C, the composition of carbon saturated fluids tends towards pure CO_2 and CH_4 becomes virtually absent. Conversely, should the user force overwhelmingly reduced conditions featuring only pure CH_4 fluid, the COH system will be left to the CH system. In the endmember situations, mathematical errors may arise from ratios leading to division by zero. In this event, the software will inform the user that the modeling cannot be pursued due to fluid being pure CO_2 or CH_4 .

4.3. Graphite/diamond precipitation

Graphite/diamond precipitation is based on Eq. (23) (see Section 2.7) as the sole precipitation reaction. More reactions could be considered, as the model strays from reality when only CO_2 or CH_4 remains present in the fluid, such as Eq. (21) involving oxidation of graphite/

diamond in CO_2 .

Computer code availability

The Thermotopes-COH software was developed by Antoine Boutier, (Dipartimento di Scienze della Terra, Università degli Studi di Torino, Via Valperga Caluso 35, 10100 Torino antoine.boutier@gmail.com, +33-644255635), under the supervision of Alberto Vitale Brovarone (Dipartimento di Scienze Biologiche, Geologiche e Ambientali, Università di Bologna, Piazza di Porta San Donato 1, 40126 Bologna; alberto.vitaleb@unibo.it). The source codes and user manual are available at <https://zenodo.org/records/10361692> under an open source license. The software is compatible with current Microsoft operating system Windows 10, and Apple Mac operating system (tested on Mojave and Catalina), and is written in Python, using Python 3.7.2. The software code makes use of the freely available package Matplotlib, Tkinter and Pandas, and has been compiled using Pyinstaller with Windows PowerShell.

Authorship statement

Category 1: Conception and design of study: Antoine Boutier, Alberto Vitale Brovarone, Coding: Antoine Boutier, Concept and features consultation: Simone Tumiati, Guillaume Siron.

Category 2: Drafting the manuscript: Antoine Boutier, Alberto Vitale Brovarone. Revising the manuscript critically for important intellectual content: Isabelle Martinez, Isabelle Daniel, Simone Tumiati, Guillaume Siron.

Category 3: Approval of the version of the manuscript to be published: Antoine Boutier, Alberto Vitale Brovarone, Isabelle Martinez, Isabelle Daniel, Simone Tumiat, Guillaume Siron.

CRedit authorship contribution statement

Antoine Boutier: Writing – review & editing, Writing – original draft, Software, Methodology, Conceptualization. **Isabelle Martinez:** Writing – review & editing, Supervision, Resources. **Simone Tumiat:** Validation, Methodology. **Guillaume Siron:** Writing – review & editing, Validation, Software, Methodology. **Alberto Vitale Brovarone:** Writing – review & editing, Writing – original draft, Visualization, Validation, Methodology, Funding acquisition.

Declaration of competing interest

The authors declare that they have no known competing financial interests or personal relationships that could have appeared to influence the work reported in this paper.

Data availability

Data will be made available on request.

Acknowledgment

Isotopic parameters come mainly from a compilation of isotopic fractionation equations from “IsoFrac” built and maintained by Jordi Delgado Martin. This work is part of a project funded by the European Research Council (ERC) under the European Union’s Horizon 2020 research and innovation program (Grant agreement No. 864045; project acronym DeepSeep). A Richard Lounsbery grant, a MIUR Rita Levi Montalcini grant, a MUR FARE grant (No. R20ZIYMPAR; acronym DRYNK), and a MUR PRIN2022 grant (No. 20224YR3AZ; acronym HYDECARB) to AVB are also acknowledged.

Appendix A. Supplementary data

Supplementary data to this article can be found online at <https://doi.org/10.1016/j.cageo.2024.105533>.

References

- Ballhaus, C., Berry, R.F., Green, D.H., 1991. High pressure experimental calibration of the olivine-orthopyroxene-spinel oxygen geobarometer: implications for the oxidation state of the upper mantle. *Contrib. Mineral. Petrol.* 107, 27–40.
- Baumgartner, L.P., Valley, J.W., 2001. Stable isotope transport and contact metamorphic fluid flow. *Rev. Mineral. Geochem.* 43, 415–467.
- Beaudoin, G., Therrien, P., 2009. The updated web stable isotope fractionation calculator. *Handb. Stable Isot. Anal. Tech.* 2, 1120–1122.
- Bebout, G.E., Fogel, M.L., 1992. Nitrogen-isotope compositions of metasedimentary rocks in the Catalina Schist, California: implications for metamorphic devolatilization history. *Geochem. Cosmochim. Acta* 56, 2839–2849.
- Berner, R.A., 1999. A new look at the long-term carbon cycle. *GSA Today (Geol. Soc. Am.)* 9, 1–6.
- Boutier, A., Martinez, I., Sissmann, O., Agostini, S., Daniel, I., Van Baalen, M., Mana, S., Brovarone, A.V., 2023. Complexity of graphite formation in response to metamorphic methane generation and transformation in an orogenic ultramafic body. *Geochem. Cosmochim. Acta*. <https://doi.org/10.1016/j.gca.2023.10.028>.
- Cesare, B., 1995. Graphite precipitation in C–O–H fluid inclusions: closed system compositional and density changes, and thermobarometric implications. *Contrib. Mineral. Petrol.* 122, 25–33.
- Connolly, J.A.D., 1995. Phase diagram methods for graphitic rocks and application to the system C–O–H–FeO–TiO₂–SiO₂. *Contrib. Mineral. Petrol.* 119, 94–116.
- Connolly, J.A.D., Cesare, B., 1993. C–O–H–S fluid composition and oxygen fugacity in graphitic metapelites. *J. Metamorph. Geol.* 11, 379–388.
- Dansgaard, W., 1964. Stable isotopes in precipitation. *Tellus* 16, 436–468.
- Dasgupta, R., 2013. Ingassing, storage, and outgassing of terrestrial carbon through geologic time. *Rev. Mineral. Geochem.* 75, 183–229. <https://doi.org/10.2138/rmg.2013.75.7>.
- Dasgupta, R., Hirschmann, M.M., 2010. The deep carbon cycle and melting in Earth’s interior. *Earth Planet. Sci. Lett.* 298, 1–13. <https://doi.org/10.1016/j.epsl.2010.06.039>.
- Day, H.W., 2012. A revised diamond-graphite transition curve. *Am. Mineral.* 97, 52–62.
- Duke, E.F., Rumble, D., 1986. Textural and isotopic variations in graphite from plutonic rocks, south-central New Hampshire. *Contrib. Mineral. Petrol.* 93, 409–419.
- Evans, K., 2011. Metamorphic carbon fluxes: how much and how fast? *Geology* 39, 95–96.
- French, B.M., 1966. Some geological implications of equilibrium between graphite and a C–H–O gas phase at high temperatures and pressures. *Rev. Geophys.* 4, 223–253.
- Frost, B.R., 2018. Introduction to oxygen fugacity and its petrologic importance. In: *Oxide Minerals*. De Gruyter, pp. 1–10.
- Galvez, M.E., Beyssac, O., Martinez, I., Benzerara, K., Chaduteau, C., Malvoisin, B., Malavieille, J., 2013. Graphite formation by carbonate reduction during subduction. *Nat. Geosci.* 6 (6), 473–477.
- Holloway, J.R., 1984. Graphite-CH₄-H₂O-CO₂ equilibria at low-grade metamorphic conditions. *Geology* 12, 455–458.
- Holloway, J.R., 1977. Fugacity and activity of molecular species in supercritical fluids. In: *Thermodynamics in Geology*. Springer, pp. 161–181.
- Huang, F., Daniel, I., Cardon, H., Montagnac, G., Sverjensky, D.A., 2017. Immiscible hydrocarbon fluids in the deep carbon cycle. *Nat. Commun.* 8, 1–8.
- Huizenga, J.M., 2005. COH, an Excel spreadsheet for composition calculations in the COH fluid system. *Comput. Geosci.* 31, 797–800.
- Kendall, C., McDonnell, J.J., 2012. *Isotope Tracers in Catchment Hydrology*. Elsevier Science Publishers, Amsterdam.
- Kitchen, N.E., Valley, J.W., 1995. Carbon isotope thermometry in marbles of the Adirondack Mountains, New York. *J. Metamorph. Geol.* 13, 577–594.
- Kokh, M.A., Akiniev, N.N., Pokrovski, G.S., Salvi, S., Guillaume, D., 2017. The role of carbon dioxide in the transport and fractionation of metals by geological fluids. *Geochem. Cosmochim. Acta* 197, 433–466.
- Luque, F.J., Crespo-Feo, E., Barrenechea, J.F., Ortega, L., 2012. Carbon isotopes of graphite: implications on fluid history. *Geosci. Front.* 3, 197–207.
- Mason, E., Edmonds, M., Turchyn, A.V., 2017. Remobilization of crustal carbon may dominate volcanic arc emissions. *Science* 357, 290–294.
- Miozzi, F., Tumiat, S., 2020. Aqueous concentration of CO₂ in carbon-saturated fluids as a highly sensitive oxybarometer. *Geochem. Persp. Lett.* 16, 30–34.
- Ohmoto, H., Kerrick, D.M., 1977. Devolatilization equilibria in graphitic systems. *Am. J. Sci.* 277, 1013–1044.
- Ortega, L., Millward, D., Luque, F.J., Barrenechea, J.F., Beyssac, O., Huizenga, J.-M., Rodas, M., Clarke, S.M., 2010. The graphite deposit at Borrowdale (UK): a catastrophic mineralizing event associated with Ordovician magmatism. *Geochem. Cosmochim. Acta* 74, 2429–2449.
- Ray, J.S., 2009. Carbon isotopic variations in fluid-deposited graphite: evidence for multicomponent Rayleigh isotopic fractionation. *Int. Geol. Rev.* 51, 45–57.
- Ray, J.S., Ramesh, R., 2000. Rayleigh fractionation of stable isotopes from a multicomponent source. *Geochem. Cosmochim. Acta* 64, 299–306.
- Rayleigh, Lord, 1896. L. Theoretical considerations respecting the separation of gases by diffusion and similar processes. *London, Edinburgh Dublin Phil. Mag. J. Sci.* 42, 493–498.
- Richet, P., Bottinga, Y., Javoy, M., 1977. A review of hydrogen, carbon, nitrogen, oxygen, sulphur, and chlorine stable isotope fractionation among gaseous molecules. *Annu. Rev. Earth Planet Sci.* 5 (1), 65–110.
- Rumble, D., Hoering, T.C., 1986. Carbon isotope geochemistry of graphite vein deposits from New Hampshire, USA. *Geochem. Cosmochim. Acta* 50 (6), 1239–1247.
- Sharp, Z., 2017. *Principles of Stable Isotope Geochemistry*, second ed. Pearson Prentice Hall. <https://doi.org/10.25844/h9q1-0p82>.
- Shi, P., Saxena, S.K., 1992. Thermodynamic modeling of the CHOS fluid system. *Am. Mineral.* 77, 1038–1049.
- Spycher, N.F., Reed, M.H., 1988. Fugacity coefficients of H₂, CO₂, CH₄, H₂O and of H₂O-CO₂-CH₄ mixtures: a virial equation treatment for moderate pressures and temperatures applicable to calculations of hydrothermal boiling. *Geochem. Cosmochim. Acta* 52, 739–749. [https://doi.org/10.1016/0016-7037\(88\)90334-1](https://doi.org/10.1016/0016-7037(88)90334-1).
- Stachel, T., Chacko, T., Luth, R.W., 2017. Carbon isotope fractionation during diamond growth in depleted peridotite: counterintuitive insights from modelling water-maximum CHO fluids as multi-component systems. *Earth Planet. Sci. Lett.* 473, 44–51.
- Stagno, V., Frost, D.J., 2010. Carbon speciation in the asthenosphere: experimental measurements of the redox conditions at which carbonate-bearing melts coexist with graphite or diamond in peridotite assemblages. *Earth Planet. Sci. Lett.* 300, 72–84.
- Taylor, B.E., Liou, J.G., 1978. The low-temperature stability of andradite in COH fluids. *Am. Mineral.* 63, 378–393.
- Taylor, W.R., Green, D.H., 1986. The role of reduced COH fluids in mantle partial melting. In: *International Kimberlite Conference: Extended Abstracts*, pp. 211–213.
- Tumiat, S., Recchia, S., Remusat, L., Tiraboschi, C., Sverjensky, D.A., Manning, C.E., Vitale Brovarone, A., Boutier, A., Spanu, D., Poli, S., 2022. Subducted organic matter buffered by marine carbonate rules the carbon isotopic signature of arc emissions. *Nat. Commun.* 13, 1–10.
- Tumiat, S., Tiraboschi, C., Miozzi, F., Vitale-Brovarone, A., Manning, C.E., Sverjensky, D.A., Milani, S., Poli, S., 2020. Dissolution susceptibility of glass-like carbon versus crystalline graphite in high-pressure aqueous fluids and implications for the behavior of organic matter in subduction zones. *Geochem. Cosmochim. Acta* 273, 383–402.
- Ulmer, P., Luth, R.W., 1991. The graphite-COH fluid equilibrium in P, T, f_{CO_2} space. *Contrib. Mineral. Petrol.* 106, 265–272.

- Valley, J.W., 1986. Stable isotope geochemistry of metamorphic rocks. *Rev. Mineral. Geochem.* 16, 445–489.
- Valley, J.W., O'Neil, J.R., 1981. $^{13}\text{C}/^{12}\text{C}$ exchange between calcite and graphite: a possible thermometer in Grenville marbles. *Geochem. Cosmochim. Acta* 45, 411–419.

- Vitale Brovarone, A., Tumiati, S., Piccoli, F., Ague, J.J., Connolly, J.A., Beysac, O., 2020. Fluid-mediated selective dissolution of subducting carbonaceous material: implications for carbon recycling and fluid fluxes at forearc depths. *Chem. Geol.* 549, 119682.